



ELSEVIER

Journal of Nuclear Materials 290–293 (2001) 935–939

**journal of
nuclear
materials**

www.elsevier.nl/locate/jnucmat

The effect of divertor magnetic balance on H-mode performance in DIII-D

T.W. Petrie^{a,*}, C.M. Greenfield^a, R.J. Grobener^a, A.W. Hyatt^a, R.J. La Haye^a,
A.W. Leonard^a, M.A. Mahdavi^a, T.H. Osborne^a, M.J. Schaffer^a,
D.M. Thomas^a, W.P. West^a, DIII-D Team, S.L. Allen^b, M.E. Fenstermacher^b,
C.J. Lasnier^b, G.D. Porter^b, N.S. Wolf^b, J.G. Watkins^c, T.L. Rhodes^d

^a DIII-D Team General Atomics, P.O. Box 85608, San Diego, CA 92186-5608, USA

^b Lawrence Livermore National Laboratory, Livermore, CA, USA

^c Sandia National Laboratories, Albuquerque, NM, USA

^d University of California, Los Angeles, CA USA

Abstract

We report on recent experiments for which the magnetic balance of highly triangular ($\delta \approx 0.8$), unpumped H-mode plasmas was varied. Changes in divertor heat loading and particle flux were observed when the magnetic configuration was varied from a balanced double-null (DN) divertor to a slightly unbalanced DN divertor. For attached plasmas, the variation in heat flux sharing between divertors is very sensitive near balanced DN. This sensitivity can be shown to be consistent with the measured scrape-off width of the parallel divertor heat flux density, $\lambda_{q_{\parallel}}$. At magnetic balance we find that the peak heat flux density at the divertor in the ∇B ion drift direction is twice that of the other divertor. Most of the heat flux go to the outboard divertor targets in a balanced double-null, where the peak heat flux density at the outer divertor targets may exceed that of the inner divertor targets by tenfold. However, the variation of the peak particle flux density between divertors is less sensitive to changes in magnetic balance. These particle and heat flux ‘asymmetries’ in DN plasmas are consistent with the presence of $E \times B$ poloidal particle drifts in the scrape-off layer and private flux region [1]. Regardless of how the divertors were magnetically balanced, D_2 gas puffing always reduced energy confinement to the range $\tau_E/\tau_{E89P} \approx 1.3$ –1.6. When this energy confinement range was reached, τ_E/τ_{E89P} remained nearly constant up to near the H-mode density limit. © 2001 Elsevier Science B.V. All rights reserved.

Keywords: Divertor asymmetry; Geometry effects; Heat flux to divertor

1. Introduction

Plasma performance in tokamaks generally improves with increased shaping of the plasma cross-section. This stronger shaping, especially higher triangularity, can produce changes in the magnetic topology of the divertor. Important engineering and divertor physics issues (e.g., power flow handling) are associated with changes

in the details of the divertor geometry, especially as the configuration transitions from a single-null (SN) divertor to a marginally balanced double-null (DN) divertor. In this paper, we examine how variation in magnetic balance affects: (1) heat flux and particle sharing by the divertors and (2) the response of the plasma confinement properties to deuterium gas fueling. To quantify the degree of ‘divertor imbalance’ (or equivalently, to what degree the shape is ‘double-null’ or ‘single-null’), we introduce a parameter $drSEP$, which we define as the radial distance between the upper divertor separatrix and the lower divertor separatrix at the outboard mid-plane. For example, if $drSEP = 0$, the configuration is a

* Corresponding author. Tel.: +1-619 455 4671; fax: +1-619 455 4156.

E-mail address: petrie@apollo.gat.com (T.W. Petrie).

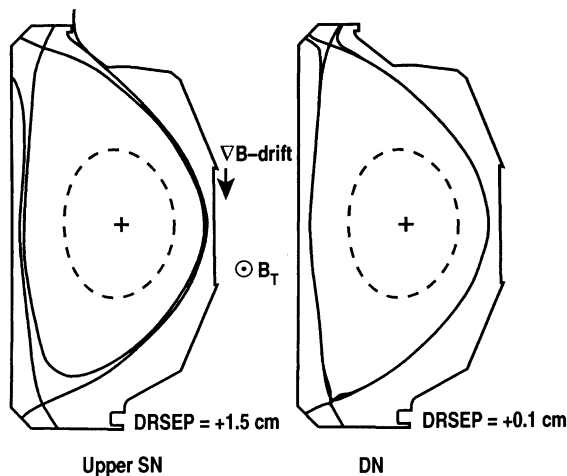


Fig. 1. Two of the plasma shapes considered in this study are shown: $drSEP = +1.5$ cm (upper SN) and $drSEP = +0.1$ cm (near-balanced DN). The direction of the toroidal field is 'out of the paper' and the direction of the plasma current is 'into the paper'. Plasma parameters: $I_p = 1.37$ MA, $B_T = 2.0$ T, $q_{95} = 4-5$, triangularity of the primary X-point = 0.78, $P_{input} = 4.5-7.0$ MW, $Z_{eff} = 1.7$, $drSEP = -4$ to $+4$ cm. No active particle pumping at the divertor strike points or in the private flux region was done for these discharges.

magnetically balanced DN; if $drSEP = +1.0$ cm, the upper divertor separatrix is innermost by 1 cm at the outer midplane. Two examples are shown in Fig. 1. The ∇B ion drift is toward the lower divertor. The experimental parameters are listed in the caption to Fig. 1.

2. Heat and particle fluxes

The peak parallel heat flux density under either outboard divertor in *attached* plasmas [2] is strongly dependent on the magnetic balance between $drSEP = -1$ and $+1$ cm (Fig. 2(a)). These data fitted to a hyperbolic tangent function, are not symmetric with respect to $drSEP = 0$. At magnetic balance, the parallel peak heat flux density at the lower divertor ($q_{||low}^p$) is approximately twice that at the upper divertor ($q_{||up}^p$). Up/down balance in the peak heat flux density occurs for $drSEP \approx 0.25$ cm. This 'offset' is observed in detached plasmas [2] as well (o), but the slope in that curve near $drSEP = 0$ is much less steep, also shown in Fig. 2(a). An 'offset' asymmetry in the peak particle flux density between upper and lower outboard (attached) divertors is shown in Fig. 2(b). Unlike the case for the heat flux density asymmetry, the peak particle flux density at the upper divertor is *higher* than that at the lower divertor at magnetic balance (Section 4). Our study indicates that uncertainty in the $drSEP$ is < 0.2 cm.

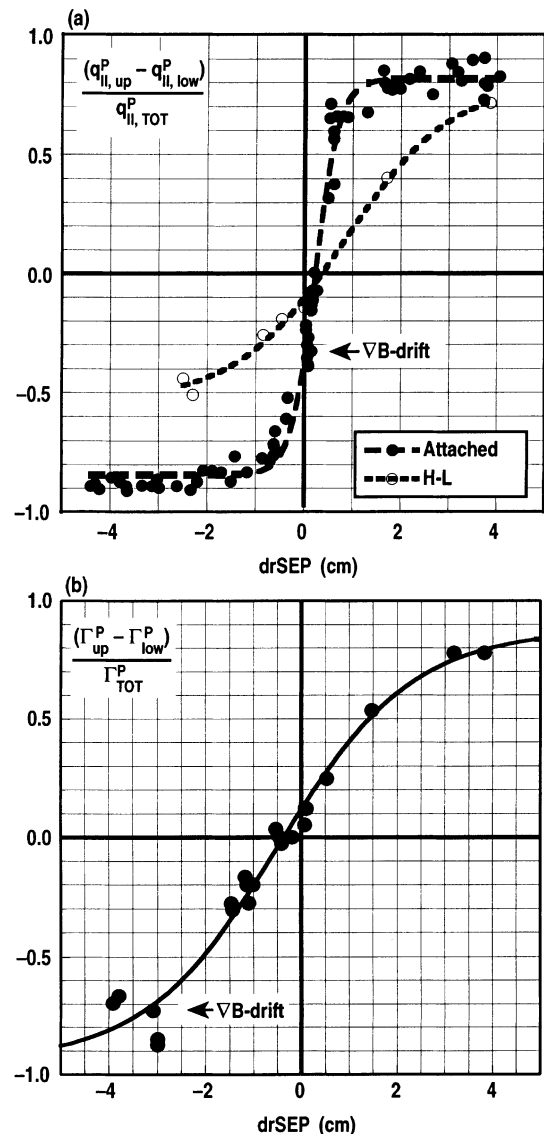


Fig. 2. (a) Peak parallel heat flux density for 'attached' divertors is roughly a factor of 2 higher in the 'lower' divertor, when the configuration is in magnetic balance (l). The peak heat flux density is balanced when $drSEP \approx 0.25$ cm. To a lesser degree, asymmetry in the peak heat flux is observed in 'detached' divertors (o). (b) There is also an asymmetry in the peak particle flux density between the upper divertor and lower divertor. $q_{||-tot}^p$ and $\Gamma_{||-tot}^p$ are the sum of the upper and lower peak parallel heat flux density and peak particle flux density, respectively. The data are fit to a hyperbolic tangent function. Uncertainty in $drSEP < 0.2$ cm.

Most of the heat is deposited at the outboard divertor targets in a balanced DN divertor (Figs. 3(a) and (b)). The ratio of the outboard-to-inboard peak heat flux density (q_{out}^p/q_{in}^p) in both upper and lower divertors is ≈ 2.5 over most of the range in $drSEP$. Near

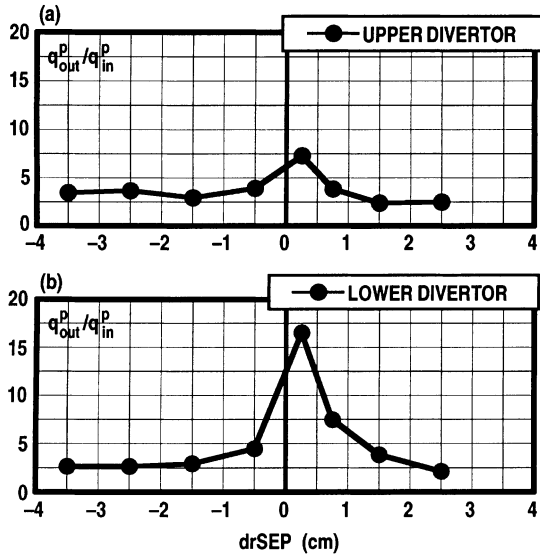


Fig. 3. The ratio of the outboard peak heat flux density to the inboard peak heat flux density at: (a) upper divertor and (b) lower divertor strike points. Measurements are made with infrared cameras.

magnetic balance, however, $q_{\text{out}}^p \gg q_{\text{in}}^p$ in both divertors. Our interpretation of these data will be presented in Section 4.

We have determined the scrape-off width, $\lambda_{q_{\parallel}}$, for the parallel heat flux density by projecting the heat flux distribution from the divertors back to the midplane using the EFITD [3] magnetic reconstruction code and the VIDDAPS [4] heat flux analysis code, and then fitting the result to an exponential function. The results, plotted in Fig. 4, show that the scrape-off width of the parallel heat flux density at the outboard midplane for attached plasmas varies between 0.4 and 0.6 cm. The squares represent $\lambda_{q_{\parallel}}$ determined by an infrared camera monitoring the lower divertor and the circles determined by an infrared camera monitoring the upper divertor. For $drSEP < 0$, $\lambda_{q_{\parallel}} \approx 0.6$ cm and for $drSEP > +2.0$ cm, $\lambda_{q_{\parallel}} \approx 0.5$ cm; $\lambda_{q_{\parallel}}$ has a minimum of ≈ 0.4 cm for $drSEP \approx +1.0$ cm. When $\lambda_{q_{\parallel}}/|drSEP| \ll 1$, $\lambda_{q_{\parallel}}$ corresponding to the primary separatrix is insensitive to $drSEP$. However, when $drSEP$ is roughly equal to $\lambda_{q_{\parallel}}$, the ‘secondary’ divertor, as expected, begins to siphon off significant power.

3. Response to gas injection

Gas puffing reduced the energy confinement of these ELMing H-mode discharges to levels where $\tau_E/\tau_{E89P} \approx 1.3$ – 1.6 , independent of the $drSEP$ value, where τ_{E89P} refers to the 1989 ITER-L-mode scaling [5]. When this

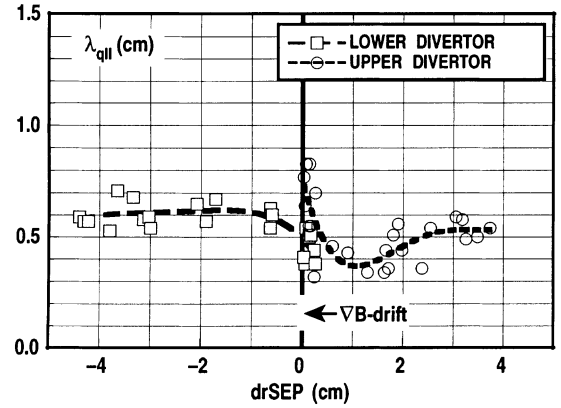


Fig. 4. The scrapeoff length ($\lambda_{q_{\parallel}}$) of the parallel heat flux density at the outboard midplane is insensitive to changes in magnetic balance, except between $drSEP = 0$ and 1 cm. Infrared camera data from the lower (\square) and upper (\circ) divertor are used. Polynomial fits to each dataset are shown. The scrapeoff profiles at the midplane are found by projecting the heat flux distribution from the divertors back to the midplane using the EFITD [3] magnetic reconstruction code and the VIDDAPS [4] heat flux analysis code.

energy confinement range was reached, τ_E/τ_{E89L} remained nearly constant during further gas puffing up to near the H–L back transition, as shown below. For these unpumped plasmas, we have not been able to fuel an ELMing H-mode plasma to high density with gas puffing only, and simultaneously maintain an energy confinement of $\tau_E/\tau_{E89P} \approx 2$.

In general, there were two distinct phases of plasma behavior during gas puffing (Fig. 5). Phase I, which covered approximately the first 0.5 s of deuterium gas puffing ($\Gamma_{D2} = 60$ Torr ℓ/s , Fig. 5(b)), was characterized by a drop in τ_E/τ_{E89P} , as well as a coincident drop in edge electron pressure $P_{e,\text{ped}}$ (Fig. 5(c)). Neither the line-averaged density \bar{n}_e nor the pedestal [6] electron density $n_{e,\text{ped}}$ increased (Fig. 5(d)). Phase II was characterized by a ‘plateau’ in τ_E/τ_{E89P} (≈ 1.4); for our data set, τ_E/τ_{E89P} lay in the range 1.3–1.6 during the ‘plateau’ phase, irrespective of $drSEP$. Note also that the ‘edge’ or pedestal electron pressure was also constant and that steady fueling of the main plasma was coincident with the start of Phase II, as evidenced by a linear rise in line-averaged density during this period.

Confinement degradation was not limited to the edge plasma. We examined the radial profiles in density and temperature at three timeslices for the shot shown in Fig. 5: (1) $t = 3.25$ s (at the start of deuterium puffing), (2) $t = 3.75$ s (start of Phase II), and (3) $t = 5.0$ s (well into the density rise during Phase II). The radial electron density profile was virtually unchanged between 3.25 and 3.75 s; steady fueling of the core plasma occurred only during Phase II. In Phase I both electron and ion

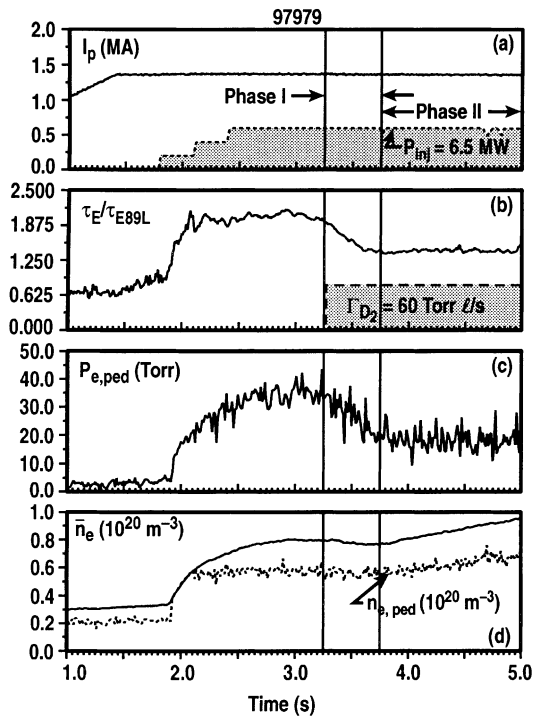


Fig. 5. Deuterium gas is injected into a lower SN divertor plasma, starting at $t = 3.25$ s. $drSEP = -3.7$ cm. Phase I: Electron energy confinement degrades with little rise in density. Phase II: Energy confinement is stable and density rises.

temperatures decreased $\approx 30\%$ in the outer region of the main plasma ($\rho/a > 0.6$) and decreased $\approx 10\text{--}25\%$ in the interior regions. During Phase II both electron and ion temperatures continued to decrease across the radial profile, but (with the rise in electron density) the plasma pressure across the profile remained approximately constant in time.

The initial decrease in energy confinement following the start of gas puffing may be mostly a consequence of increased ion transport, as determined from ONETWO transport code [7] analysis. This analysis also indicates that electron conductivity did not change appreciably during Phase I for $\rho < 0.7$. Ion conductivity, however, increased by about a factor of 2–4 across the entire profile during this time. While the electron conductivity inside the $q = 2$ flux surface was still considerably higher than the ion conductivity by the end of Phase I, the ion conductivity rose to comparable values with electron conductivity outboard of the $q = 2$ surface. Stacey has analyzed this shot from an edge plasma stability perspective [8] and has concluded that this increase in ion conductivity (but not in electron conductivity) may be caused by short radial wavelength thermal instabilities in the ion channel, driven by radiation and atomic physics at the edge [9].

4. Discussion

The observed heat and particle flux asymmetries may be driven by $E \times B$ poloidal drifts. This is suggested by experiments and modeling of SN plasmas. For example, $E \times B$ poloidal particle flows across the private flux region (PFR) were measured in DIII-D divertor plasmas and found to be in agreement with the particle flow predicted by modeling [1,10]. At present, the modeling of these symmetry-breaking particle drifts in the DN configuration is only at a rudimentary level for available 2D fluid modeling edge transport codes, such as UEDGE [11]. Yet, the fact that 2D fluid modeling (UEDGE) has been used successfully to study the importance of $E \times B$ drifts in the less complicated (SN) configurations gives confidence that our basic understanding of $E \times B$ edge plasma drifts is grounded well enough to hypothesize what these drifts might be doing in the DNs. (Other ‘classical’ drifts [12] may also contribute to the observed asymmetries and these will be addressed in future work.)

Up/down asymmetries DN. The origin of the electric field (E) which may drive the drift in the PFR, arises mainly from the radial gradient in the electron temperature with respect to the flux surfaces in the PFR and its direction is always into the PFR. The direction of the toroidal field B is shown in Fig. 1. Thus, the direction of the $E \times B$ poloidal flow in the lower divertor is from the outboard leg to the inboard leg across the PFR. On the other hand, in the upper divertor, the direction of this flow is from the inboard divertor leg to the outboard divertor leg. In a balanced DN divertor, including these $E \times B$ drifts would lead to a higher particle flux density at the upper outboard (UO) divertor target than at the lower outboard (LO) divertor target, as seen in the experiment (Fig. 2(b)). This asymmetry in peak particle flux density implies higher particle density at the UO and lower inboard (LI) targets, as compared with the LO and upper inboard (UI) targets, respectively. In turn, this higher density, taken together with an assumption of constant plasma pressure along field lines connecting the respective upper and lower divertors, results in lower electron temperatures (T_e) and lower heat flux density for LI versus UI and UO versus LO, where we take $q_{||}^p \propto n_e \times T_e^{1.5}$. Thus, in a magnetically balanced case, we expect a heat flux density asymmetry to be biased toward the LO divertor in comparison with the UO divertor. With the same set of arguments, the higher density and lower T_e at the LI target (compared with the UI target) also lead to lower heat flux density at the LI target (compared with the UI target). Preliminary UEDGE modeling of a DIII-D-like DN discharge [13] qualitatively supports this interpretation.

Out/in asymmetries in DN. The same set of arguments can be applied to in/out asymmetry. The higher density and lower T_e at the LI target (compared with the UI

target) also lead to lower heat flux density at the LI target (compared with the UI target). With the result in the above paragraph, we would expect the out/in ratio to be higher in the lower divertor than in the upper divertor (as observed). Based *only* on ‘geometric’ arguments, we would expect some out/in peak heat flux asymmetries in both upper and lower divertors for balanced DNs. First, the radial gradients of density and temperature on the low field (outboard) side are about twice those of the high field (inboard) side. Second, the ratio of plasma surface area outboard of the separatrices to the area inboard of the separatrices is approximately 1.7 for the configurations considered in this study. If we assume that the diffusivities are poloidally uniform and we then relate $q_{\text{out}}^{\text{p}}$ and $q_{\text{in}}^{\text{p}} \propto \chi \cdot \nabla_r \cdot T \cdot \text{Area}$, we estimate the in/out heat flux ratio $\approx 3\text{--}4$. This estimate is somewhat less than the measured ratios (i.e. $q_{\text{out}}^{\text{p}}/q_{\text{in}}^{\text{p}} \approx 8\text{--}20$).

Cooling from radiated power along the inboard and outboard divertor legs could account for some of the discrepancy between measured and predicted out/in heat flux ratio. (Radiated power measurements to the required accuracy were not available during these experiments for quantitative analysis.) A second possibility that could increase the out/in heat flux asymmetry is turbulent transport on the weak field side of the core plasma [14,15]. ‘Poor’ curvature on the outboard side of the X-points and ‘good’ curvature on the inboard side can enhance the power flow losses through the weak field side. For DNs, this ‘enhanced’ power loss on the weak field side is directed into the outboard divertors and is cut off from the inboard divertors. Divertor heating on the inboard side must then rely on the less lossy transport on the strong field side. Thus, this ‘severing’ of the inboard and outboard transport in DNs could enhance $q_{\text{out}}^{\text{p}}/q_{\text{in}}^{\text{p}}$ over the simple geometric predictions discussed above. While this interpretation is still at the hypothesis stage, reflectometer fluctuation measurements of the outboard midplane made during this experiment gives some support to it, i.e., an increase in density fluctuation amplitude, as the plasma goes from an unbalanced to magnetic configuration (and conversely, a decrease in fluctuation amplitude in going from balanced to unbalanced configuration).

5. Summary and conclusions

We have shown that the peak heat flux density balance (up/down and in/out) is highly sensitive to variation in magnetic balance near the double-null configuration in attached plasmas, and this sensitivity is characterized

by the scrapeoff width of the parallel heat flux density at the outboard midplane $\lambda_{q_{\parallel}}$. Our data are consistent with the $E \times B$ poloidal drift playing an important role in these observed asymmetries, although other ‘classical’ drifts may also impact our results. The strong in/out heat flux asymmetries for DNs may relax the cooling requirements for handling the power flowing to the inboard divertors sufficiently to allow active cooling of the inboard divertors and simplify the engineering of the inboard divertor. This reduced cooling need would be an advantageous feature for high triangularity, low aspect ratio tokamaks [16]. Particle flux to the outboard divertors is less sensitive to changes in magnetic balance. This implies that magnetic balance control may be less critical to particle pumping. Degradation of τ_E with gas injection was seen for all values of $drSEP$.

Acknowledgements

The work was supported by the U.S. Department of Energy under Contract Nos. DE-AC03-99ER54463, W-7405-ENG-48, DE-AC04-94AL85000, and Grant No. DE-FG03-86ER53225.

References

- [1] T.D. Rognlien et al., J. Nucl. Mater. 266-269 (1999) 654.
- [2] T.W. Petrie et al., Nucl. Fus. 37 (1997) 321.
- [3] L.L. Lao et al., Nucl. Fus. 25 (1985) 1611.
- [4] C.J. Lasnier et al., Nucl. Fus. 38 (1998) 1225.
- [5] P.N. Yushmanov et al., Nucl. Fus. 30 (1990) 1999.
- [6] R.J. Groebner, T.H. Osborne, Phys. Plasmas 5 (1998) 1800.
- [7] W.W. Pfeiffer, ONETWO: a computer code for modeling plasma transport in Tokamaks, General Atomics Report GA-A16178, 1980.
- [8] W.M. Stacey, Phys. Plasmas 6 (1999) 2452.
- [9] W.M. Stacey, T.W. Petrie, Phys. Plasmas 7 (2000) 4931.
- [10] J.A. Boedo et al., Phys. Plasmas 7 (2000) 1075.
- [11] T.D. Rognlien et al., Plasma Phys. 34 (1994) 362.
- [12] A.V. Chankin, J. Nucl. Mater. 241–243 (1997) 199.
- [13] M. Rensink, private communication.
- [14] G.R. Tynan, On the Origins of Tokamak Edge Turbulence and the H-mode Transition, Advanced Series in Nonlinear Dynamics, vol. 9, World Scientific, Singapore, 1995, p. 254.
- [15] X. Xu et al., in: Proceedings of the 13th U.S. Transport Task Force (TTF) Workshop, Burlington, Vermont, April 2000 pp. 26–29.
- [16] K.M. Morel, G.F. Counsell, P. Helander, J. Nucl. Mater. 266–269 (1999) 1040.